Dynamic Optimization of Functionally Graded Thin-Walled Box Beams

Article *in* International Journal of Structural Stability and Dynamics · February 2017

DOI: 10.1142/S0219455417501097

1 author:

Karam Maalawi
National Research Center, Egypt
75 PUBLICATIONS **847** CITATIONS

International Journal of Structural Stability and Dynamics
Vol. 17, No. 9 (2017) 1750109 (24 pages)

DOI: 10.1142/S0219455417501097

Dynamic Optimization of Functionally Graded Thin-Walled Box Beams

Karam Y. Maalawi

Department of Mechanical Engineering
National Research Centre
P.O. 12622 Dokki, Cairo, Egypt
nrc.aero@gmail.com

Received 14 August 2016
Accepted 21 December 2016
Published 6 February 2017

This paper introduces a mathematical model for optimizing the dynamic performance of thin-walled functionally graded box beams with closed cross-sections. The objective function is to maximize the natural frequencies and place them at their target values to avoid the occurrence of large amplitudes of vibration. The variables considered include fiber volume fraction, fiber orientation angle and ply thickness distributions. Various power-law expressions describing the distribution of the fiber volume fraction have been implemented, where the power exponent was taken as the main optimization variable. The mass of the beam is kept equal to that of a known reference beam. Side constraints are also imposed on the design variables in order to avoid having unacceptable optimal solutions. The mathematical formulation is carried out in dimensionless quantities, enabling the generalization to include models with different cross-sectional types and beam configurations. The optimization problem is solved by invoking the *MatLab* optimization *ToolBox* routines, along with structural dynamic analysis and eigenvalue calculation routines. A case study on the optimization of a cantilevered, single-cell spar beam made of carbon/epoxy composite is considered. The results for the basic case of uncoupled bending motion are given. Conspicuous design charts are developed, showing the optimum design trends for the mathematical models implemented in the study. It is concluded that the natural frequencies, even though expressed in implicit functions, are well-behaved, monotonic and can be treated as explicit functions in the design variables. Finally, the developed models can be suitably used in the global optimization of typical composite, functionally graded, thin-walled beam structures.

Keywords: Structural dynamics; optimum design; thin-walled box beams; functionally graded materials.

1. Introduction

Many applications of structural design optimization to different problems have been given in the literature.[1] One interesting problem in aerospace industry is the optimization of the airplane wing structure through maximization of the *stiffness-to-mass*

ratio under strength and stability constraints. Figure 1 shows a typical wing panel with both the exterior aerodynamic surface and the interior main load-carrying spar box beam structure. The latter is usually made of composite thin-walled constructions which can be suitable candidates for aeronautical structures. They offer the advantage of achieving high *stiffness-to-mass* ratio besides producing desirable modes of deformation through elastic tailoring. Extension-twist and bending-twist couplings can be produced by the anisotropy of the material. Such couplings can be relevant for wing optimization where even relatively small changes in the angle of attack could result in significant changes in airloads.[2]

Several studies have been addressed for the structural analysis and optimization of composite beams. Cardoso and Valido[3] applied nonlinear programming techniques to optimize cross-sectional properties of composite, thin-walled beams. The main design variables included laminate thickness and fiber orientation angles. The optimal composite box-beam structure was also addressed in Ref. 4 where the objective function was measured by maximizing failure margins subject to strength constraints. Ply orientation angle was taken as a main design variable, and Tsai–Wu–Haln failure criterion was applied to calculate the reserve factor for each wall and ply. Ferrero *et al.*[5] presented a simple analytical theory for determining stiffness and stress of thin-walled beams subjected to twisting moment. They showed that their results correlate accurately with those obtained from 3D finite element modeling. Another work by Banerjee and Su[6] introduced a novel solution technique for analyzing the free bending vibration of beams with torsional coupling. It was shown that the proposed theory can be applied to a wide range of problems including aircraft wings.

A new class of composite materials can be produced by varying the volume fractions of their constituents in a predetermined profile. Such nonuniform

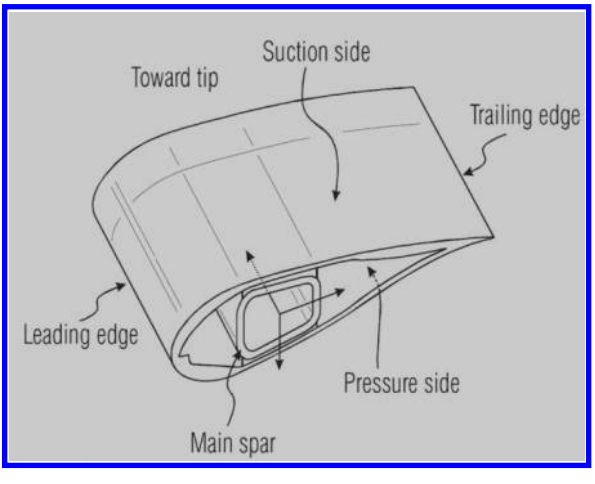

Fig. 1. Typical panel of an airplane wing structure.

composites are called functionally graded materials (FGMs) in which the properties are functions of the spatial coordinates. Basic knowledge on the use of FGMs and their wide applications are given in Suresh and Mortensen.[7] FGMs were primarily used in situations where large temperature gradients are encountered. Applications related to stability and dynamic of FGM structures are outlined by Birman and Byrd[8] who presented a comprehensive review of the development of FGMs.

A recent work dealing with divergence and flutter of a spinning FGM cantilevered pipe subjected to an axial force at the free end and a high temperature environment is presented by Eftekhari and Hosseini.[9] The effect of changing the volume fraction of the FGM through the wall thickness is considered in formulating the needed stability map of the pipe structure. The material properties vary continuously across the pipe thickness from being fully metal at the inner surface of the pipe to being fully ceramic at the outer surface. It was found that the volume fraction distribution plays an important role on the stability regions of the spinning system. Another work by George *et al.*[10] studied buckling and vibration behavior of FGM carbon nanotube reinforced polymer composite plate. Four different functionally graded distributions have been considered and compared. The physical and mechanical properties are determined using the rule of mixture with the inclusion of efficiency factors to account for the geometry of the reinforced tubes. It was observed that the functional grading of the carbon nanotube can have significant influence on the buckling mode shapes and natural frequencies as well. A grading model named grade-X type has resulted in the highest values of the plate natural frequencies. In another paper by Fan and Shao,[11] exponential distributions of material properties have been addressed to study the torsional mode for thin cylindrical shell used as FGM piezoelectric energy harvester. The effect of the functionally graded parameters on the power density were investigated and discussed.

In the field of the optimum design of FGM structures, Librescu *et al.*[12] considered problems related to thermo-elastic modeling and behavior of thin-walled beams made of FGMs. They applied a simple power-law distribution for the composition of the material phases across the beam wall thickness. Effects of the transverse shear, warping and pretwist of the beam cross-section along its span were included in the model formulation. Another work was given by Maalawi,[13] developing an analytical approach for designing efficient patterns of FGM bars having maximized frequencies while maintaining the total mass at a constant value. The distribution of the volume fractions of the material constituents was optimized using either discrete or continuous variations along the bar length.

In this study, the *MatLab* optimization routines coupled with structural analysis and eigenvalue calculation routines are implemented to solve the formulated nonlinear optimization problem. Design variables include the fiber volume fraction, ply angle and thickness. As a case study, the developed mathematical model is applied to optimize a cantilevered, thin-walled spar beam made of carbon/epoxy composites. Results have indicated that the approach applied in this study can be efficient in

obtaining optimized designs in a reasonable computer time. Actually, the suggested model has succeeded in finding the needed optimal solutions indicating significant improvements in the targeted design goal as compared with a reference beam.

2. Structural Dynamic Analysis

Figure 2 shows a slender, composite thin-walled beam constructed from uniform segments. Each of which has different cross-sectional dimensions, material properties and length. Tapered shapes of an actual wing spar can be adequately approximated by such a piecewise structural model with a sufficient number of segments.

The various parameters and variables are normalized with respect to a reference beam, which is constructed from just one segment with single unidirectional lamina having equal fiber and matrix volume fractions, i.e. $V_{\text{fo}} = V_{\text{mo}} = 50\%$. The different quantities are defined in the following:

N_s = Number of segments (panels).
j = subscript for the jth segment, $j = 1, 2, \ldots, Ns$
$N_L(j)$ = Number of layers in the jth segment.
k = subscript for the kth layer, $k = 1, 2, \ldots, N_L(j)$
$\hat{L}_j = (L_j/L_o)$ = Normalized length of the jth segment.
$\hat{L} = (L/L_o) = \sum_{j=1}^{N_s} \hat{L}_j$ = Normalized total beam length.
$\widehat{H}_j = (H_j/H_0) = \widehat{H}_j = \sum_{k=1}^{N_L(j)} \hat{h}_{kj}$ = Normalized total wall thickness of the jth segment.

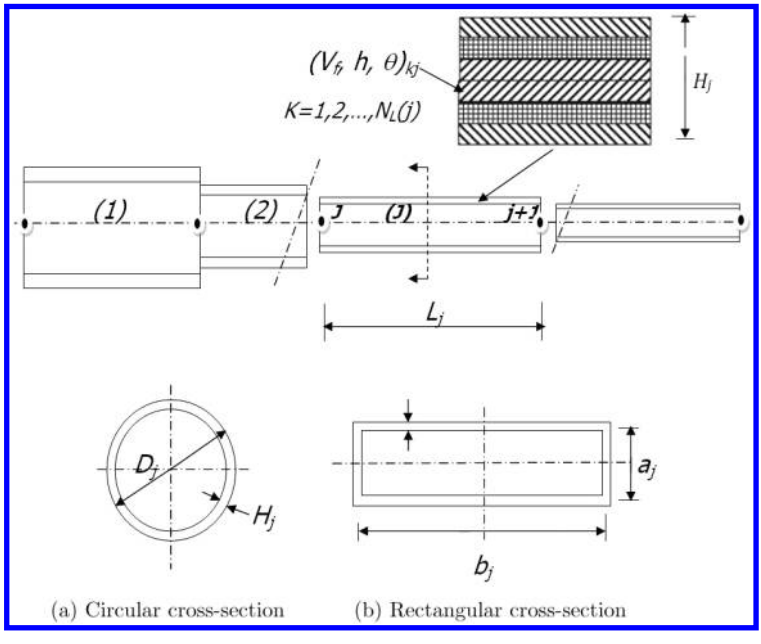

Fig. 2. General configuration of a multi-segment, composite box beam.

$\hat{h}_{kj} = (h_{kj}/H_0)$ = Normalized thickness of the kth layer in the jth segment.
θ_{kj} = Fiber orientation angle in the kth layer in the jth segment.
$\hat{\Gamma}_j = \Gamma_j/\Gamma_o = \oint_J ds/\oint_o ds$ = Normalized circumference of the jth segment cross-section.
$\Gamma_j = \pi D_j$ for circular $C.S.$, $\Gamma_j = 2(a_j + b_j)$ for rectangular $C.S.$
$\hat{\rho}_{kj} = \rho_{kj}/\rho_o$ = Normalized density of the kth layer in the jth segment.
$V_{f,kj}$ = Fiber volume fraction in the kth layer in the jth segment.
$\rho_{kj} = \rho_f V_{f,kj} + \rho_m(1 - V_{f,kj})$, $\rho_o = 0.5(\rho_f + \rho_m)$
ρ_f = fiber mass density, ρ_m = matrix density
$\hat{m}_j = (m_j/m_o)$ = Normalized mass per unit length of the jth segment.
$m_j = \Gamma_j \sum_{k=1}^{N_L(j)} \rho_{kj} h_{kj}$ = Mass per unit length of the jth segment, $m_o = \Gamma_o \rho_o H_o$.
I_j = mass polar moment of inertia per unit length of the jth segment.

$$= \sum_{k}^{N_L(j)} \oint \rho_{kj} h_{kj}(y^2 + z^2) ds.$$

The normalized total structural mass is given by the expression:

$$\hat{M}_s = M_s/M_0 = \sum_{j=1}^{N_s} \hat{M}_j = \sum_{j=1}^{N_s} \hat{m}_j \hat{L}_j = \sum_{j=1}^{N_s} \hat{\Gamma}_j \hat{L}_j \sum_{k=1}^{N_L(j)} \hat{\rho}_{kj} \hat{h}_{kj}, \tag{1}$$

where $M_o = m_o L_o = \Gamma_o \rho_o H_o L_o$ is the total mass of the uniform baseline design.

A quantity with subscript "o" refers to a baseline design parameter.

2.1. *Constitutive relationships*

The displacement field of anisotropic thin-walled closed-cross-sectional beams was derived by Armanios and Badir,[14] who used a variational asymptotic approach. A brief of the basic assumptions, equations and notations will be reviewed in the following.

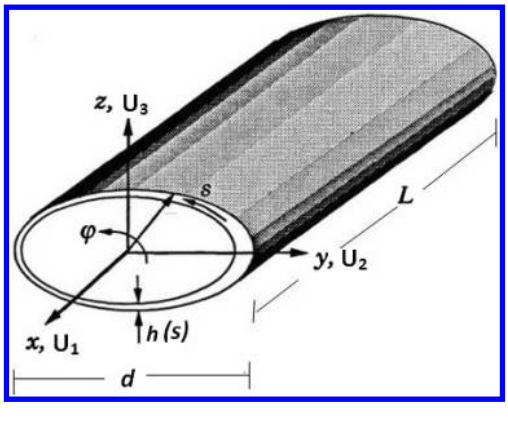

Fig. 3. Coordinate systems and kinematic variables.[14]

Considering the composite cylindrical shell model shown in Fig. 3, it is assumed that the geometric dimensions are such that

$$d \ll L, \quad h \ll d \tag{2}$$

where d stands for the maximum cross-sectional dimension, L for the axial length and h for the maximum value of the wall thickness. The material properties are allowed to vary both in the circumferential and thickness directions. The shell thickness is also allowed to change in the s-direction. The notations U_1, U_2, U_3 and φ are the kinematic variables representing the average displacements and rotation of the cross-section as indicated in Fig. 3. At any point of the cross-section, the displacements can be expressed as

$$\begin{aligned} u_1(x,s) &= U_1(x) - y(s)U_2'(x) - z(s)U_3'(x) + g(sx), \\ u_2(x,s) &= U_2(x) - z(s)\varphi(x), \\ u_3(x,s) &= U_3(x) + z(s)\varphi(x). \end{aligned} \tag{3}$$

The primes denote differentiation with respect to x. The function $g(s,x)$ added to the classical displacement field of extension, bending and torsion represents the out-of-plane warping of the cross-section. The constitutive equations are given by the following matrix equation:

$$\begin{Bmatrix} F_x \\ M_x \\ M_y \\ M_z \end{Bmatrix} = \begin{bmatrix} C_{11} & C_{12} & C_{13} & C_{14} \\ C_{12} & C_{22} & C_{23} & C_{24} \\ C_{13} & C_{23} & C_{33} & C_{34} \\ C_{14} & C_{24} & C_{34} & C_{44} \end{bmatrix} \begin{Bmatrix} U_1' \\ \varphi' \\ U_3'' \\ U_2'' \end{Bmatrix}, \tag{4}$$

where F_x, M_x, M_z and M_y stand for the axial force, bending and torsional moments, respectively. C_{mn} are the cross-sectional stiffness coefficients derived in terms of closed form integrals of the geometry and material constants (see Appendix A).

2.2. *Equations of motion*

The equations of motion for the free vibration analysis are derived using Hamilton's principle. The expression of the strain energy is given by

$$\begin{aligned} U &= \frac{1}{2}\int_0^L \{q\}^T[C][q]dx, \\ \{q\}^T &= \{\, U_1' \quad \varphi' \quad U_3'' \quad U_2'' \,\}, \end{aligned} \tag{5}$$

and the kinetic energy density per unit length is

$$K \cong \oint \int_{-h/2}^{+h/2} \frac{1}{2}\rho[\dot{U}_1 + (\dot{U}_2 - z\dot{\varphi})^2 + (\dot{U}_3 + y\dot{\varphi})^2 d\zeta ds, \tag{6}$$

where ρ is the material density and the dot denotes differentiation with respect to time, t. Applying Hamilton's principle

$$\int_{t_1}^{t_2}\int_0^L \delta(K-U)dxdt = 0 \tag{7}$$

the resulting equations of motion in terms of the kinematic variables are

$$\begin{aligned}
C_{11}U_1'' + C_{12}\varphi'' + C_{13}U_3''' + C_{14}U_2''' - m\ddot{U}_1 = 0,\\
C_{12}U_1'' + C_{22}\varphi'' + C_{23}U_3''' + C_{24}U_2''' - I\ddot{\varphi} - S_z\ddot{U}_3 + S_y\ddot{U}_2 = 0,\\
C_{13}U_1''' + C_{23}\varphi''' + C_{33}U_3'''' + C_{34}U_2'''' + S_z\ddot{\varphi} + m\ddot{U}_3 = 0,\\
C_{14}U_1''' + C_{24}\varphi''' + C_{34}U_3'''' + C_{44}U_2'''' - S_y\ddot{\varphi} + m\ddot{U}_2 = 0.
\end{aligned} \tag{8}$$

The parameters associated with the inertia terms in Eq. (8) are defined as

$$\begin{aligned}
m &= \oint \rho h(s)ds,\\
I &= \oint \rho(y^2+z^2)h(s)ds,\\
S_y &= \oint \rho z h(s)ds,\\
S_z &= \oint \rho y h(s)ds.
\end{aligned} \tag{9}$$

A closed-form solution of Eq. (8) is not available. However, particular choices of cross-sectional shape and lay-up can produce zero coupling coefficients in the equations of motion. References 14 and 15 considered two lay-up configurations, namely, Circumferentially Asymmetric Stiffness (CAS) and Circumferentially Uniform Stiffness (CUS), as depicted in Fig. 4.

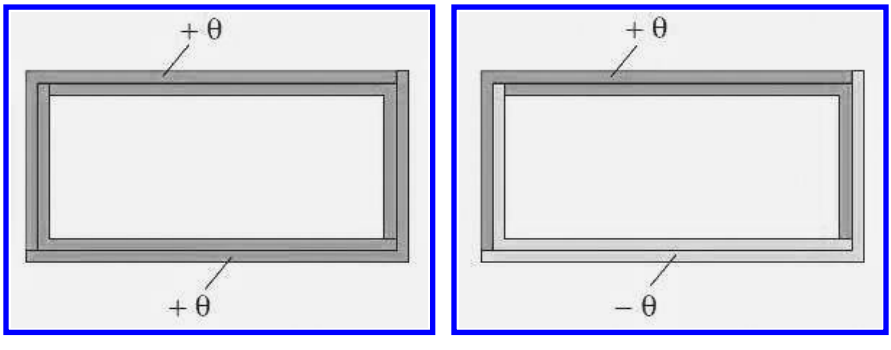

(a) (b)

Fig. 4. Special lay-up configurations (ply angle θ measured about the outward normal axis). (a) CUS "Helical lay-up" (extension/twist coupling) and (b) CAS "Mirror lay-up" (bending/twist coupling).

The reduced equations of motion are given in the following:
(a) CUS lay-up

$$\begin{aligned} C_{11}U_1'' + C_{12}\varphi'' - m\ddot{U}_1 &= 0, \\ C_{12}U_1'' + C_{22}\varphi'' - I\ddot{\varphi} &= 0, \\ C_{33}U_3'''' + m\ddot{U}_3 &= 0, \\ C_{44}U_2'''' + m\ddot{U}_2 &= 0 \end{aligned} \tag{10}$$

which consist of two coupled equations for extension-twist and two uncoupled bending equations. Superscript dot denotes derivative with respect to time.
(b) CAS lay-up

$$\begin{aligned} &C_{11}U_1'' - m\ddot{U}_1 = 0, \\ &C_{22}\varphi'' + C_{23}U_3'''' - I\ddot{\varphi} = 0, \\ &C_{23}\varphi''' + C_{33}U_3'''' + m\ddot{U}_3 = 0, \\ &C_{44}U_2'''' + m\ddot{U}_2 = 0, \end{aligned} \tag{11}$$

where the extension displacement (U_1) is uncoupled, as well as the edgewise bending (U_2), while the flatwise bending (U_3) is coupled with twist (φ).

3. Solution Procedure

Dancila and Armanios[15] presented the exact solutions of Eqs. (10) and (11) for a cantilevered thin-walled beam with constant cross-sectional dimensions and material properties along its length. The solutions for the uncoupled axial and bending equations are straightforward, while those for the coupled equations involved much mathematics. The general solution of the homogeneous equations of motion can be obtained by separating the space and time variables, where the time dependence is assumed to be harmonic with circular frequency, ω. For the CUS configuration, the closed-form solution obtained by Dancila and Armanios[15] is summarized in the following:

$$\omega_k = \frac{(2k+1)\pi}{2L}\sqrt{\frac{2a}{b \pm \Delta}}, \quad k = 0, 1, 2, \ldots, \tag{12a}$$

$$\text{where :} \quad a = C_{11}C_{22} - C_{12}^2, \quad b = C_{11}I + C_{22}m, \quad c = mI, \quad \Delta = \sqrt{b^2 - 4ac}. \tag{12b}$$

Three conditions are given:

- if $C_{11}I > C_{22}m$, the –ve sign will generate frequencies for the axial-mode dominated vibrations, while the +ve sign will generate frequencies for torsionally dominated vibrations.
- If $C_{11}I < C_{22}m$, the roles are reversed.
- If $C_{11}I = C_{22}m$, the natural frequencies can be assigned to either type of mode, the values being numerically equal.

For the CAS configuration, the closed-form solution for the bending-twist vibrations cannot be obtained. However, for a specific cross-sectional dimensions and material properties, numerical solutions are obtained using a PC-based version of the computer code Mathematica. The code allows for both symbolic manipulation and numerical computation with arbitrary precision.[15]

3.1. *Uncoupled bending motion*

The basic important case to be considered first is the uncoupled bending response, which exists in both CUS and CAS lay-up configurations. Using the multi-segment model depicted in Fig. 2 and considering flatwise bending (U_3), the associated eigenvalue problem can be written directly in the form:

$$C_{33,j}U_3'''' - \omega^2 m_j U_3 = 0 \tag{13}$$

which must be satisfied over the length L_j of any segment composing the beam structure (see Fig. 2). For specific shapes of the beam cross-section, the stiffness coefficient $C_{33,j}$ can be easily determined as follows (refer to Fig. 2 and Appendix A).

$$\begin{aligned} C_{33,j} &= \frac{1}{6}a_j^2(a_j + 3b_j)\left(A - \frac{B^2}{C}\right) \quad \text{for rectangular C.S.} \\ &= \frac{\pi D_j^3}{8}\left(A - \frac{B^2}{C}\right) \quad \text{for circular C.S.} \end{aligned} \tag{14}$$

3.2. *Variation of fiber volume fraction (V_f)*

There are different scenarios in modeling the spatial variation of material properties of a functionally graded structure. For example, Chen and Gibson[18] considered distributions represented by polynomial functions, and applied Galerkin's method to calculate the required polynomial coefficients from the resulting algebraic equations. They found that the linear variation of the volume fraction is a best fit with that predicted experimentally for selected composite beam specimens. Chi and Chung[19] studied the mechanical behavior of FGM plates under transverse loading, where a constant Poisson's ratio and variable moduli of elasticity throughout the plate thickness was assumed. The volume fraction of the constituent materials were defined by simple power-laws, and closed form solutions using Fourier series were given for the case of simply- supported plates. The distribution of the material properties in functionally graded structures may be designed by either continuous or piecewise variation of the volume fraction in a specified direction. Bedjilili *et al.*[20] considered vibration of fibrous composite beams with a variable volume fraction through the thickness of the cross-section. The utilized power-law expression is given as

$$v_f(\hat{z}) = v_f(0) + [v_f(0.5) - v_f(0)](2|\hat{z}|)^P, \quad -0.5 \le \hat{z}\left(=\frac{z}{h}\right) \le 0.5, \quad p \ge 0. \tag{15}$$

Upper and lower bounds are imposed on the volume fraction of the fiber to be within a prescribed range for consideration of other strength and manufacturing requirements. Another type of power-law model was implemented by Librescu and Maalawi[21] who investigated aeroelastic optimization of composite wings using the concept of material grading in the spanwise direction by applying the expression:

$$v_f(\hat{x}) = v_{fr}(1 - \beta_f \hat{x}^P), \quad 0 \le \hat{x}\left(= \frac{x}{L}\right) \le 1, \quad \beta_f = (1 - \Delta_f), \quad \Delta_f = v_{ft}/v_{fr}, \quad (16)$$

where v_{ft} and v_{fr} are the fiber volume fractions at wing tip and root, respectively. Δ_f is called the tapering ratio of the fiber volume fraction. A more general distribution was tried by Shih-Yao[22] who applied it successfully to investigate the effect of grading on the supersonic flutter of rectangular composite plates. The utilized power-law formula is

$$v_f(\hat{x}) = v_{fr}[\beta_f(1 - \hat{x}^n)^p + \Delta_f], \quad n = 1, 2, 3 \; p \ge 0. \quad (17)$$

3.3. *Frequency equation*

Normalizing Eq. (13) with respect to the baseline design, we get

$$\widehat{U}_3'''' - \hat{\beta}_j^4 \widehat{U}_3 = 0, \quad (18)$$

where $\hat{\beta}_j = \sqrt{\widehat{\omega}}(\hat{m}_j/\hat{C}_{33,j})^{1/4}$, $\hat{C}_{33,j} = C_{33,j}/C_{33,0}$, and $\widehat{\omega} = \omega L_0^2(\frac{m_0}{C_{33,0}})^{1/2}$. Equation (18) must be satisfied in the interval $0 \le \bar{x} \le \hat{L}_j$, where $\bar{x} = \hat{x} - \hat{x}_j$ is a local coordinate of the jth segment and $\hat{x} = (x/L_o)$. The general solution is well known to be[16]:

$$\hat{U}_3(\bar{x}) = a_1 \sin \hat{\beta}_j \bar{x} + a_2 \cos \hat{\beta}_j \bar{x} + a_3 \sinh \hat{\beta}_j \bar{x} + a_4 \cosh \hat{\beta}_j \bar{x}. \quad (19)$$

Expressing the constants a_i, $i = 1, 2, 3, 4$ in terms of the state variables vector $\{S\}^T = \{U_3 - U_3' - C_{33}U_3'' - C_{33}U_3'''\}^T$ at both ends of the jth segment, we get

$$\{S\}_{j+1} = [T^{(j)}]\{S\}_j, \quad (20)$$

where $[T^{(j)}]$ is called the transfer matrix of the jth segment (refer to Appendix B). The state variable vectors can be computed progressively along the length of the beam by applying continuity among the interconnecting joints of the different segments composing the beam structure. An overall transfer matrix denoted by $[T]$, which relates the state variables at both ends of the beam, can be obtained from the following matrix multiplication:

$$[T] = [T^{(Ns)}][T^{(Ns-1)}] \cdots [T^{(2)}][T^{(1)}]. \quad (21)$$

The required frequency equation for determining the natural frequencies can then be obtained by applying the associated boundary conditions and considering only the nontrivial solution of the resulting matrix equation.

4. Formulation of the Optimization Problem

Several design objectives can exist in structural optimization including minimum mass, maximum natural frequencies, minimum manufacturing cost, etc. Maalawi and El-Chazly[23] presented optimization models for beam structures considering both stability and dynamic performance. They applied mathematical programming coupled with finite element analysis procedures. Another crucial issue is the reduction or control of the vibration level. Two optimization alternatives for vibration reduction can be formulated, namely, frequency placement by separating the natural frequencies from the harmonics of the excitations or direct maximization of the natural frequencies. The latter can ensure a simultaneous balanced improvement in both of stiffness and mass distributions of the vibrating structure. The related optimization problems are usually formulated as nonlinear mathematical programming problem[24] where iterative techniques are implemented for finding the optimal solution in the selected design space.

4.1. *Maximization of natural frequencies*

The first alternative of the objective function form is represented by a direct maximization of a weighted-sum of the natural frequencies which is expressed mathematically as follows:

$$\begin{aligned} &\text{Minimize } F(\underline{X}) = -\sum_i \alpha_i \hat{\omega}_i, \\ &\sum_i \alpha_i = 1, 0 \le \alpha_i \le 1, \end{aligned} \tag{22}$$

where $\hat{\omega}_i$ are the normalized frequencies, α_i weighting factors measuring the relative importance of each frequency and $\underline{X}$ is the chosen design variables vector encompassing fiber volume fraction, ply angle and thickness. The outside dimensions of the beam cross-section are restricted by the outer aerodynamic shape of the wing and will be considered as preassigned parameters in the present model formulation.

4.2. *Frequency placement criterion*

Frequency placement can be achieved by minimizing a weighted-sum of the squares of the difference between each frequency $\hat{\omega}_i$ and its target or desired value $\hat{\omega}_i^*$, i.e.,

$$\text{Minimize } F(\underline{X}) = \sum_i \alpha_i (\hat{\omega}_i - \hat{\omega}_i^*)^2. \tag{23}$$

Both objectives in Eqs. (22) and (23) are subject to the constraints:

$$\text{Mass constraint} : \hat{M}_s = 1, \tag{24a}$$

$$\text{Side constraints} : \underline{X}_L \le \underline{X} \le \underline{X}_U, \tag{24b}$$

where $\underline{X}_U$ and $\underline{X}_L$ are the upper and lower bounds set on the values of the variables vector $\underline{X}$ to avoid having unacceptable designs in the attained optimal solutions.

Approximate values of the desired frequencies are usually selected to be within narrow bands, sometimes called frequency-windows, of those corresponding to an initial beam design. Such values are adjusted to be different from the critical exciting frequencies. Numerous computer programs[1] are available to solve the proposed optimization model, which can be interacted with structural and eigenvalue analyses routines. Different types of unconstrained and constrained optimization algorithms are included in the powerful *MATLAB* toolbox optimization routines.[25] "*fmincon*" is one of the most commonly applied routines that finds the constrained optima of a merit function of many variables (refer to Appendix C for details).

4.3. *Basic optimization problem*

Before performing the necessary mathematics, it is essential to recognize that design optimization is only as meaningful as its core model of structural analysis. Any deficiencies therein will absolutely be affected in the optimization process. Consider the basic problem of a uniform cantilevered, thin-walled, beam constructed from just one segment with one unidirectional lamina ($Ns = 1$, $N_L = 1$). In this case, the associated frequency equation is

$$\cos\hat{\beta}\hat{L}\cosh\hat{\beta}\hat{L} = -1, \text{ or} \tag{25a}$$

$$\cos\sqrt{\widehat{\omega}}(\widehat{m}/\hat{C}_{33})^{\frac{1}{4}}\hat{L}\cosh\sqrt{\widehat{\omega}}(\widehat{m}/\hat{C}_{33})^{\frac{1}{4}}\hat{L} = -1. \tag{25b}$$

It is seen that $\sqrt{\widehat{\omega}}$ is an implicit function of the design variables and can be calculated numerically by any suitable method such as Newton–Raphson or the Bisection method. However, the frequency equation can be solved directly for the whole term $\sqrt{\widehat{\omega}}(\widehat{m}/\hat{C}_{33})^{\frac{1}{4}}\hat{L}$ without regard to the specific values of the design variables. The computed roots are

$$\sqrt{\widehat{\omega}} = (\widehat{C}_{33}/\hat{m})^{\frac{1}{4}}\left(\frac{1}{\widehat{L}}\right)(1.8751, 4.6941, 7.8548, \ldots, \pi[i-0.5])i \geq 4. \tag{26}$$

In Eq. (26), the frequency parameter $\sqrt{\widehat{\omega}}$ can be imagined as an explicit function of the design variables. So, for prescribed values of the design variables within the domain of side constraints $\sqrt{\widehat{\omega}}$ can be obtained directly from the above equation. Therefore, it is possible to place the frequency at its desired value and obtain the corresponding value of any one of the design variables directly from Eq. (26).

5. Case Studies and Discussions

The mathematical models developed above have been applied to obtain the required optimal solutions of a cantilevered, thin-walled, single cell, composite spar beam. The selected composite material of construction is made of epoxy-3501-6 and carbon-AS4 (see Table 1) which has favorable properties and is highly recommended in many applications of civil, aerospace and mechanical engineering.[17]

Table 1. Material properties of fiber and matrix materials*.

Property	Carbon-AS4 fiber	Epoxy-3501-6
Density (g/cm^3)	$\rho_f = 1.81$	$\rho_m = 1.27$
Modulus of elasticity (GPa)	$E_{1f} = 235.0$	$E_m = 4.30$
	$E_{2f} = 15.0$	
Modulus of rigidity (GPa)	$G_{12f} = 27.0$	$G_m = 1.60$
Poisson's ratio	$\nu_{12f} = 0.20$	$\nu_m = 0.35$

Notes: *For a final structural design, experimental verifications are necessary.[17]

Two different forms of the objective function measuring frequency optimization have been defined in Eqs. (22) and (23). It is useful to investigate first the functional behavior of the natural frequencies and examine their variation with the chosen design variables while maintaining the total mass constant.

5.1. *One-segment spar beam*

First, we consider the basic case of a one-segment ($N_s = 1$), one-layer ($N_L = 1$) cantilevered beam. The total length and outer cross-sectional-dimensions are given preassigned values equal to those of the baseline design. The remaining set of variables is, therefore, $\underline{X} = (V_f, \widehat{H}, \theta)$. The imposed side constraints are

$$\begin{aligned} &0.25 \le V_f \le 0.75, \\ &0.75 \le \widehat{H} \le 1.25, \\ &-\pi/2 \le \theta \le \pi/2. \end{aligned} \tag{27}$$

A couple of words are stated here regarding the side constraints in Eq. (27). First of all, it is reminded that the main focus of the present study is to optimize the fiber volume fraction in order to achieve higher values of the natural frequencies without mass penalty. The optimization is performed with respect to a known baseline design which is considered to be conservative having reserve strength to withstand severe dynamic loads. The imposed side constraint on the total wall thickness, normalized with respect to that of the baseline design, is included for consideration of strength and stability requirements which are not considered in the present study. So, the imposed limits with a percentage of 25% below or above that of the baseline can be practically accepted for the given model formulation. A simplified example considering static stress and deflection constraints is given in Appendix C. On the other hand, appropriate values of the upper and lower bounds imposed on the fiber volume fraction are chosen to avoid having unacceptable designs from the manufacture point of view. For example, the filament winding is usually associated with the highest fiber volume fractions. With careful control of fiber tension and resin content, values of around 75% would be reasonable.[27]

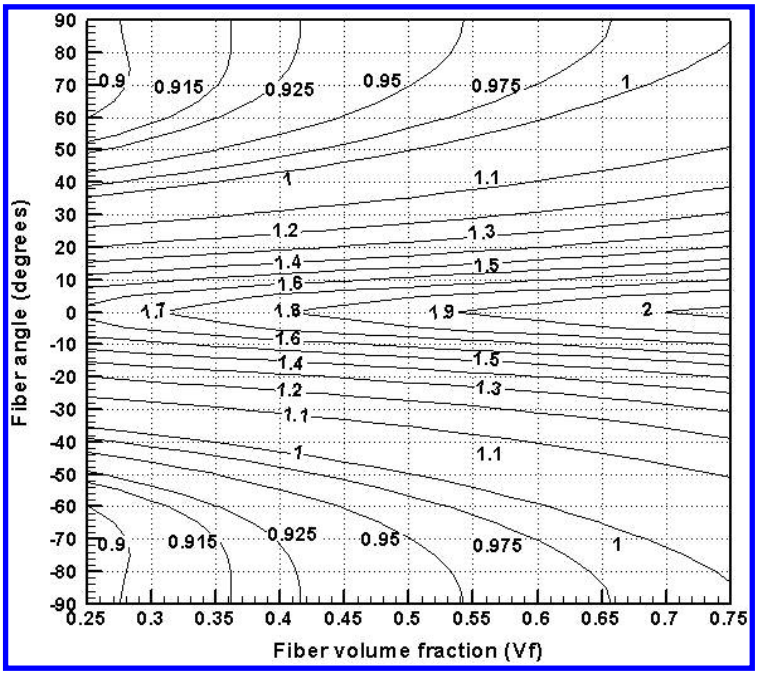

Fig. 5. Level curves of $\sqrt{\widehat{\omega}_1}$-function augmented with the equality mass constraint $\widehat{M}_s = 1$ in $(V_f - \theta)$ design space. One-segment cantilevered spar beam ($N_L = 1$, $\hat{L} = \hat{D} = 1$).

Figure 5 depicts the functional behavior of the dimensionless fundamental frequency parameter $\sqrt{\widehat{\omega}_1}$ combined with the structural mass constraint. It is remarked that the function is continuous and well behaved everywhere in $(V_f - \theta)$ design space. The contours are symmetric about the horizontal line $\theta = 0$ where the constrained global maxima occurs when the fiber volume fraction reaches its upper limiting value. It can then be concluded that the unidirectional lamina is favorable when considering beam designs with maximum bending frequency. The optimal design point was found to be $(V_f, \widehat{H}, \theta) = (0.75,\ 0.92,\ 0)$ at which $(\sqrt{\omega_1})_{\max} = 2.02589$. This corresponds to an optimization gain of about 8.04% as measured from the reference value 1.8751. Before ending this section, it is interesting to address here the dual optimization problem of minimizing the total structural mass under preserved frequency ($\sqrt{\widehat{\omega}_1} = 1.8751$). The optimal solution was calculated to be $(V_f, \widehat{H}, \theta) = (0.50,\ 0.915,\ 0)$ and $\widehat{M}_{s,\min} = 0.915$ which corresponds to a mass saving of 8.5% as compared to the baseline design.

5.2. *Two-segment spar beam*

Next, a two-segment, spar beam, which is made of one unidirectional lamina, is analyzed (see Fig. 6). The reduced optimization problem is cast in the

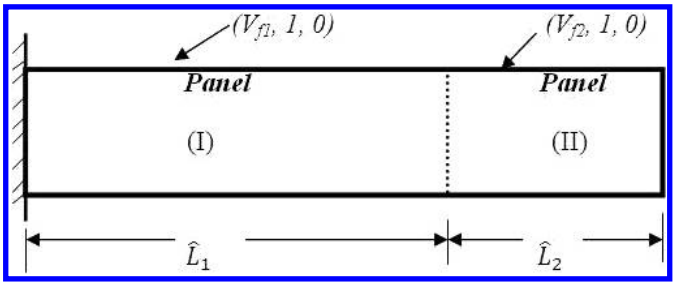

Fig. 6. Two-segment, one unidirectional lamina spar beam.

following:

$$\begin{aligned}
&\text{Minimize } F(\underline{X}) = -(\sqrt{\widehat{\omega}_1}),\\
&\text{Subject to } \widehat{M}_s = 1,\\
&\sum_{1}^{Ns} \hat{L}_j = 1,\\
&0.25 \le V_{fj} \le 0.75 \quad j = 1, 2,\\
&0.0 \le \hat{L}_j \le 1.0 \quad j = 1, 2.
\end{aligned} \tag{28}$$

Using the equality constraints, two of the design variables can be expressed in terms of the other two variables. Figure 7 shows the functional behavior of the dimensionless frequency combined with the structural mass constraint. It is remarked that the function is well defined in the feasible domain of the selected design space $(V_A - \hat{L})_1$. Two empty regions can be observed at the upper left and right parts of the design space, where violation of the equality mass constraint is indicated. In the left one, the fiber volume fraction is equal to 100%, violating the imposed side constraint. The feasible domain is seen to be split into two distinct zones separated by the baseline contour, which is represented by the vertical line $V_{f1} = 50\%$. The constrained optimum is to found to be: $(V_{fj}, \hat{L}_j)_{j=1,2} = (0.75, 0.50)$, $(0.25,\ 0.50)$ corresponding to $(\sqrt{\widehat{\omega}_1})_{\max} = 2.0645$ with 10.10% optimization gain.

5.3. *Optimal distribution of volume fractions*

For continuous grading models, the associated optimization problem is cast in the following:

Find the design variables vector $\underline{X} = (\Delta_f, p)$ which minimizes the objective function

$$F(\underline{X}) = -\sqrt{\widehat{\omega}_1},$$

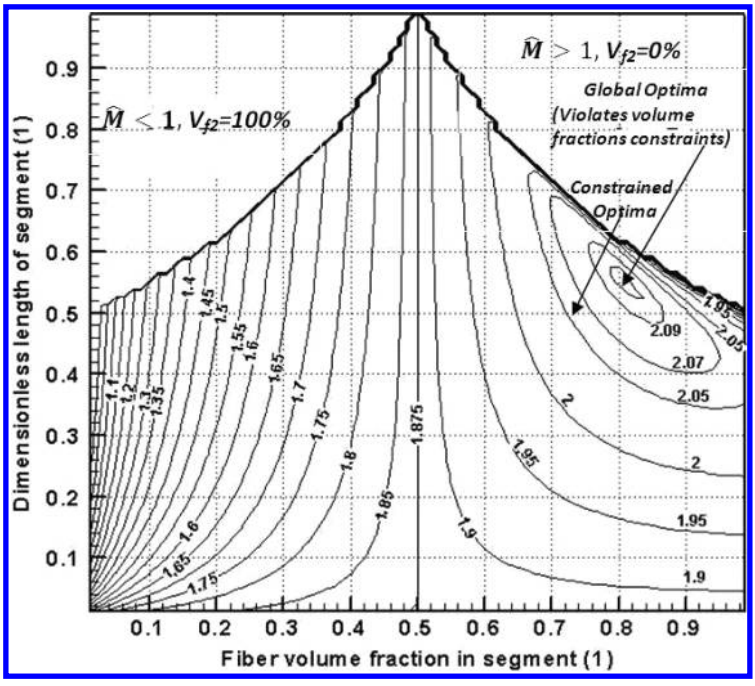

Fig. 7. Level curves of $\sqrt{\widehat{\omega}_1}$-function augmented with the equality mass constraint $\widehat{M}_s = 1$ in $(V_{f1}, \hat{L}_1)$ design space. Two-segment cantilevered spar beam.

subject to the constraints

$$\begin{gathered} \widehat{M}_s = 1, \\ 0.33 \leq \Delta_f \leq 3.0, \\ P \geq 0. \end{gathered} \tag{29}$$

Solutions obtained by applying the power-law model of Eq. (15) have shown that no improvements can be achieved using grading of the fiber volume fraction in the thickness direction. On the other hand, grading in spanwise direction has shown some interesting results. Considering spanwise grading according to Eq. (16), Fig. 8 depicts the level curves of the fundamental frequency parameter $\sqrt{\widehat{\omega}_1}$ combined with the mass constraint in the design space (Δ_f, p). It is observed that the feasible domain is bounded from below and above by the constraint curves corresponding to the upper and lower bounds imposed on the fiber volume fractions at tip and root. The horizontal line $\Delta_f = 1.0$ (i.e. $V_f = 50\%$ at root and tip) split the domain into two zones. The lower zone encompasses the constrained optimum solution: $(\sqrt{\widehat{\omega}_1})_{\max} = 2.01875$ at the design point $(\Delta_f, P)_{\text{opt.}} = (0.34, 1.01)$.

Table 2 summarizes the attained optimal solutions for the different grading patterns. It is seen that the highest optimization gain is obtained by using spanwise grading of Eq. (17) with the coordinate exponent $n = 3$.

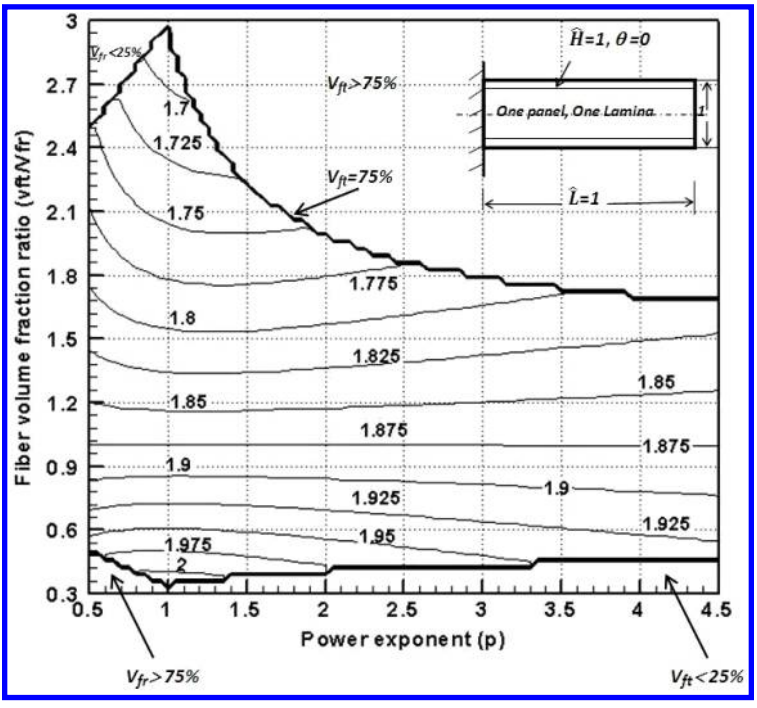

Fig. 8. Level curves of $\sqrt{\widehat{\omega}_1}$-function augmented with the equality mass constraint $\widehat{M}_s = 1$ in (Δ_f, p) design space. One-segment, one unidirectional lamina spar beam with spanwise grading of fiber volume fraction "Eq. (16)".

Table 2. Optimal solutions using different grading patterns ($\widehat{M}_s = 1$).

V_f-power-law model		$(\Delta_f, p)_{\text{opt.}}$, $(\sqrt{\omega_1})_{\max}$, Gain %
Thickness grading (Eq. (15))		(1.0, 0.0), 1.8751 0.0%
Spanwise grading (Eq. (16))		(0.34, 1.01), 2.01875, 7.66%
Spanwise grading (Eq. (17))	$n = 1$	(0.34, 1.02), 2.01938, 7.70%
	$n = 2$	(0.34, 2.425), 2.04813, 9.23%
	$n = 3$	(0.34, 5.175), 2.06125, 9.93%

6. Conclusions

Appropriate optimization models have been formulated and presented for improving the dynamic performance and increasing the overall stiffness-to-mass level of thin-walled composite beams. The objective function has been measured by maximizing the natural frequencies under mass constraint. Design variables include the distribution of volume fraction, ply angle and thickness. For discrete models, the optimized beams can be constructed from any arbitrary number of uniform segments where the length of each segment has shown to be an important variable in the optimization process. It has also been proved that expressing all parameters in dimensionless forms results in naturally scaled design variables, constraints and

objective function which is favored by a variety of optimization algorithms. The attained optimal solutions using continuous grading depend entirely upon the prescribed power-law expression which represents additional constraint on the optimization problem. For the case of uncoupled bending motion, there were no improvements achieved when applying grading in thickness direction. Results from the present formulation shows that discrete grading of material properties can be promising producing better designs with enhanced dynamic performance. In conclusion, a useful approach has been presented by constructing suitable objective functions and utilizing nonlinear programming techniques to the formulated optimum design problem. Current investigations include both cases of coupled bending/torsion and extension/torsion motions. Relevant potential areas such as optimization of FGM plates shall be investigated in future studies.

Appendix A

The stiffness coefficients C_{mn} in Eq. (4) are[14,15]

$$
\begin{aligned}
C_{11} &= \oint\left(A-\frac{B^2}{C}\right)ds+\frac{\left[\oint(\frac{B}{C})ds\right]^2}{\oint(\frac{1}{C})ds},\\
C_{12} &= \frac{\oint(\frac{B}{C})ds}{\oint(\frac{1}{C})ds}A_e,\\
C_{13} &= -\oint\left(A-\frac{B^2}{C}\right)zds-\frac{\oint(\frac{B}{C})ds\oint(\frac{B}{C})zds}{\oint(\frac{1}{C})ds},\\
C_{14} &= -\oint\left(A-\frac{B^2}{C}\right)yds-\frac{\oint(\frac{B}{C})ds\oint(\frac{B}{C})yds}{\oint(\frac{1}{C})ds},\\
C_{22} &= \frac{1}{\oint(\frac{1}{C})ds}A_e^2,\\
C_{23} &= -\frac{\oint(\frac{B}{C})zds}{\oint(\frac{1}{C})ds}A_e,\\
C_{24} &= -\frac{\oint(\frac{B}{C})yds}{\oint(\frac{1}{C})ds}A_e,\\
C_{33} &= \oint\left(A-\frac{B^2}{C}\right)z^2ds+\frac{\left[\oint(\frac{B}{C})zds\right]^2}{\oint(\frac{1}{C})ds},\\
C_{34} &= \oint\left(A-\frac{B^2}{C}\right)yzds+\frac{\oint(\frac{B}{C})yds\oint(\frac{B}{C})zds}{\oint(\frac{1}{C})ds},\\
C_{44} &= \oint\left(A-\frac{B^2}{C}\right)y^2ds+\frac{\left[\oint(\frac{B}{C})yds\right]^2}{\oint(\frac{1}{C})ds},
\end{aligned}
\tag{A.1}
$$

where A_e is the enclosed area of the cross-section and the parameters A, B and C are called the reduced axial, coupling and shear stiffness, respectively. They are

expressed in terms of the laminate in-plane stiffnesses A_{mn} by the relations[17]

$$\begin{aligned} A &= A_{11} - A_{12}^2/A_{22}, \\ B &= 2(A_{16} - A_{12}A_{26}/A_{22}), \\ C &= 4(A_{66} - A_{26}^2/A_{22}), \end{aligned} \tag{A.2}$$

$$A_{mn} = H_o \sum_{k=1}^{N_L(j)} \bar{Q}_{mn}^{(k)} \hat{h}_{kj}; \quad m, n = 1, 2, 6, \tag{A.3}$$

where $\bar{Q}_{mn}^{(k)}$ are the elements of the kth lamina stiffness matrix, which depend upon the ply angle and mechanical properties of the composite material.

A variety of approaches have been developed to predict the mechanical properties of fibrous composite materials.[17] The common approaches fall into the following general categories:

(1) Mechanics of materials.
(2) Numerical methods.
(3) Variational approach.
(4) Semi-empirical.
(5) Experimental.

Mechanics of materials approach is based on simplifying assumptions of either uniform strain or uniform stress in the constituents. Its predictions can be adequate only for longitudinal properties of unidirectional continuous fibrous composites. Numerical methods using finite difference, finite element, or boundary element methods yield the best predictions; however, they are time consuming and do not yield closed-form expressions. Variational methods based on energy principles have been developed to establish bounds (inequality relations) on the effective properties. The bounds are close to each other in the case of longitudinal properties, but they can be far apart in the case of transverse and shear properties. Semi-empirical relationships have been developed to avoid the difficulties with the above theoretical approaches and to facilitate computations. The so-called Halpin–Tsai relationships have consistent forms for all properties of fibrous composite materials.

Table A.1 gives the mathematical expressions of the various elastic moduli, which are based on the empirical methods suggested by Halpin–Tsai.[17] The volume fractions and type of the matrix and fiber materials have to be assigned.

Table A.1. Halpin–Tsai semi-empirical relations.[17]

Elastic property mathematical formula	
$E_{11} = E_m V_m + E_{1f} V_f$	
$E_{22} = E_m\ (1 + \xi\eta V_f)/(1 - \eta V_f)$	$\eta = (E_{2f} - E_m)/(E_{2f} + \xi E_m)$
$G_{12} = G_m\ (1 + \xi\eta V_f)/(1 - \eta V_f)$	$\eta = (G_{12f} - G_m)/(G_{12f} + \xi G_m)$
$\nu_{12} = \nu_m V_m + \nu_{12f} V_f$	

G_{12} denotes the shear modulus, ν_{12} the major Poisson's ratio and E_{22} and E_{11} are the Young's moduli in the principal material directions. V denotes volume fraction. Subscripts "m" and "f" denote properties of matrix and fiber materials, respectively. The sum $V_m + V_f = 1$, assuming no voids are present.

The factor ξ is a measure of reinforcement of the composite material that depends on the fiber geometry, packing geometry and loading conditions.[26] It is used to make Halpin–Tsai relations conform to the experimental data. The two theoretical extremes that bound the composite properties E_{22} and G_{12} are

$$\text{For } \xi \to 0 \quad \frac{1}{E_{22}} = \frac{V_m}{E_m} + \frac{V_f}{E_{2f}} \quad \text{and for } \xi \to \infty \quad E_{22} = E_m V_m + E_{2f} V_f. \tag{A.4}$$

The same applies to G_{12}. Whitney[26] suggested the range $1 < \xi < 2$ depending on the fiber array type, e.g. hexagonal, square, etc. Usually, ξ is taken equal to 1.0 for theoretical analysis procedures in the case of carbon or glass fibrous composite laminates.

Appendix B

The elements of the transfer matrix of any segment "j" are (see Fig. 2 and Eq. (20)):

$$T_{11} = T_{22} = T_{33} = T_{44} = \frac{1}{2}(C_j + Ch_j), \quad T_{12} = -T_{34} = -\frac{1}{2\hat{\beta}_j}(S_j + Sh_j),$$

$$T_{13} = -T_{24} = \frac{1}{2\hat{C}_{33,j}\hat{\beta}_j^2}(C_j - Ch_j), \quad T_{31} = -T_{42} = \frac{1}{2}\hat{C}_{33,j}\hat{\beta}_j^2(C_j - Ch_j),$$

$$T_{21} = -T_{43} = -\frac{1}{2}\hat{\beta}_j(S_j - Sh_j), \quad T_{14} = \frac{1}{2\hat{C}_{33,j}\hat{\beta}_j^2}(S_j - Sh_j),$$

$$T_{23} = \frac{1}{2\hat{C}_{33,j}\hat{\beta}_j}(S_j + Sh_j), \quad T_{32} = -\frac{1}{2}\hat{C}_{33,j}\hat{\beta}_j(S_j - Sh_j),$$

$$T_{41} = -\frac{1}{2}\hat{C}_{33,j}\hat{\beta}_j^3(S_j + Sh_j),$$

where

$$C_j = \text{Cos}(\hat{\beta}_j\hat{L}_j) \quad Ch_j = \text{Cosh}(\hat{\beta}_j\hat{L}_j) \quad S_j = \text{Sin}(\hat{\beta}_j\hat{L}_j) \quad Sh_j = \text{Sinh}(\hat{\beta}_j\hat{L}_j)$$

$$\hat{\beta}_j = \sqrt{\hat{\omega}}\left(\frac{\hat{m}_j}{\hat{C}_{33,j}}\right)^{\frac{1}{4}}; \quad \sqrt{\hat{\omega}} = \left(\frac{m_0}{C_{33,o}}\right)^{\frac{1}{4}} L_0\sqrt{\omega}$$

Appendix C

C.1. *Optimization with MATLAB programming*

MATLAB, which means *MATrix LABoratory*, is a powerful tool for advanced mathematics, engineering and science research.[25] Its optimization toolbox is a collection of functions consisting of *M*-files that extend the capability of *MATLAB*

numeric computing environment. The toolbox includes many routines for different types of optimization encompassing both unconstrained and constrained minimization algorithms.[24] One of the useful *MATLAB* routines is named "*fmincon*" which attempts to find the constrained minimum of an objective function of several variables starting at an initial estimate. This is generally referred to as constrained nonlinear optimization or nonlinear programming. Its general form is

$$\begin{aligned} &\min f(x) \quad \text{subject to} \\ &C(x) \leq 0, \\ &C_{\text{eq}}(x) = 0, \\ &A \cdot x \leq b, \\ &A_{\text{eq}} \cdot x = b_{\text{eq}}, \\ &lb \leq x \leq ub, \end{aligned} \tag{C.1}$$

where x, b, b_{eq}, lb, and ub are vectors, A and A_{eq} are matrices, $C(x)$ and $C_{\text{eq}}(x)$ are functions that return vectors, and $f(x)$ is a function that returns a scalar. $f(x)$, $c(x)$, and $c_{\text{eq}}(x)$ can be nonlinear functions.

C.2. *Structural optimization with MatLab: An illustration*

As an illustration, the minimal weight design of a simple I-beam structure is given herein. Figure C.1 shows the beam model, which is used as a horizontal member in a fixed E-series gantry crane. The hoist, with a capacity $W = 2000$ *Ib*, is at the middle of the beam.

Material properties: density $\rho = 0.284$ *Ib*/in^3, modulus of elasticity $E = 29 \times 10^6$ psi, tensile yield strength $\sigma_y = 36 \times 10^3$ psi, shear strength $\tau_y = 21 \times 10^3$ psi.

The associated optimization problem is cast in the following:

Find the design variable vector $\underline{x} = \{x_1, x_2, x_3, x_4\}$ which minimizes the total structural weight representing the objective function:

$$f(\underline{x}) = \rho L(2x_2x_4 + x_1x_3 - 2x_3x_4), \tag{C.2}$$

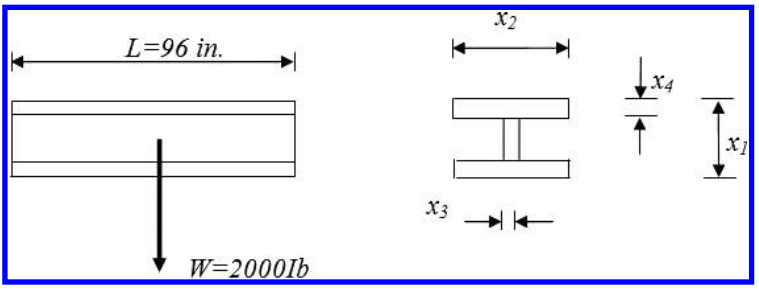

Fig. C.1. Definition of I-beam design optimization variables.

subject to the behavioral constraints:

$$\begin{aligned} &\text{Normal stress} &&: (\sigma_{\max}/\sigma_{\text{allow}}) - 1.0 \le 0, \\ &\text{Shear stress} &&: (\tau_{\max}/\tau_{\text{allow}}) - 1.0 \le 0, \\ &\text{Lateral deflection} &&: (\delta_{\max}/\delta_{\text{allow}}) - 1.0 \le 0, \end{aligned} \tag{C.3}$$

and the geometrical and side constraints:

$$\begin{aligned} &x_1 - 3x_2 \le 0; \quad 2x_2 - x_1 \le 0; \quad x_3 - 1.5x_4 \le 0; \quad 0.5x_4 - x_3 \le 0 \\ &\quad 3 \le x_1 \le 20; \quad 2 \le x_2 \le 15; \quad 0.125 \le x_3 \le 0.75; \quad 0.25 \le x_4 \le 1.25. \end{aligned} \tag{C.4}$$

The allowable normal, σ_{allow}, and shear, τ_{allow}, stresses can be determined by dividing the corresponding yielding strengths by a factor of safety, which was taken as 1.4. The allowable deflection, δ_{allow}, was specified a value of 0.25 in. The maximum stresses $\sigma_{\max}$, $\tau_{\max}$ and the maximum deflection, $\delta_{\max}$ can be calculated by using the basic equations of strength of materials.

$$\begin{aligned} \sigma_{\max} &= WL.x_1/8I; \quad \tau_{\max} = WQ/2Ix_3; \quad \delta_{\max} = WL^3/48EI, \\ I &= [x_2x_1^3 - (x_2 - x_4)(x_1 - 2x_3)^3]/12, \\ Q &= 0.5(x_1 - x_4)(x_2x_4 + x_3(x_1 - x_4)). \end{aligned} \tag{C.5}$$

MatLab Code: The code contains three m-files.
(1) The objective function m-file **ibeamobj.m**

```
% Objective function
function f=ibeamobj(x)
f=27.264*(2*x(2)*x(4)+x(1)*x(3)-2*x(3)*x(4));
```

(2) The constraint functions m-file **ibeamconf.m**

```
% Constraint functions
function [c,ceq]=ibeamconf(x)
c=[657.018-29*(x(2)*x(1)^3-(x(2)-x(4))*(x(1)-2*x(3))^3);...
   5.75-x(2)*x(1)^3 +(x(2)-x(4))*(x(1)-2*x(3))^3; ...
   6*(x(2)*x(4)*(x(1)-x(4))+x(3)*(x(1)-x(4))^2)-21*x(3)*(x(2)*x(1)^3-(x(2)-x(4))
*(x(1)-2*x(3))^3); ...
    x(1)-3*x(2);2*x(2)-x(1);x(3)-1.5*x(4);0.5*x(4)-x(3)];
ceq=[];
```

(3) The fmincon function m-file **ibeamo.m**

```
type ibeamobj
type ibeamconf
% Lower bounds
lb=[3 2 0.125 0.25];
% Upper bounds
ub=[20 15 0.75 1.25];
% Starting design
```

```
X0=[5.0 2.0 0.2 0.25];
options = optimset('LargeScale','off');
[X, fval, exitflag, output] = fmincon(@ibeamobj,x0,[],[],[],[],lb,ub,@ibeamconf,
options);
X
fval
[c, ceq] = ibeamconf(x)
output.funcCount
```

Solution: $x_1 = 4.3752$ $x_2 = 2.0$ $x_3 = 0.125$ $x_4 = 0.25$ f(x)=40.4705.

References

1. K. Y. Maalawi and M. A. Badr, Design optimization of mechanical elements and structures: A review with application, *J. Appl. Sci. Res.* **5**(2) (2009) 221–231.
2. Na Sungsoo, J.-S. Song, J.-H. Choo and Z. Qin, Dynamic aeroelastic response and active control of composite thin-walled beam structure in compressible flow, *J. Sound Vibr.* **330**(21) (2011) 4998–5013.
3. J. B. Cardoso and A. J. Valido, Cross-Section optimal design of composite laminated thin-walled beams, *Comput. Struct.* **89** (2011) 1069–1076.
4. R. Kathiravan and R. Ganguli, Strength design of composite beam using gradient and particle swarm optimization, *Compos. Struct.* **81** (2007) 471–479.
5. J. F. Ferrero, J. J. Barrau, J. M. Segura, B. Castanie and M. Sudre, Torsion of thin-walled composite beams with midplane symmetry, *Compos. Struct.* **54** (2001) 111–120.
6. J. R. Banerjee and H. Su, Free transverse and lateral vibration of beams with torsional coupling, *J. Aerosp. Eng. ASCE* (2006) 13–20.
7. S. Suresh and A. Mortensen, *Fundamentals of Functionally Graded Materials* (Cambridge University Press, UK, 1998).
8. V. Birman and W. L. Byrd, Modeling and analysis of functionally graded materials and structures, *Appl. Mech. Rev.* **60**(5) (2007) 195–216.
9. M. Eftekhari and M. Hosseini, On the stability of spinning functionally graded cantilevered pipes subjected to fluid-thermomechanical loading, *Int. J. Struct. Stab. Dyn.* **16**(9) (2016) 1–26.
10. N. George, P. Jeyaraj and S. M. Murigendrappa, Buckling and free vibration of nonuniformly heated functionally graded carbon nanotube reinforced polymer composite plate, *Int. J. Struct. Stab. Dyn.* **17**(6) (2017) 1–32.
11. T. Fan and X. Shao, Functionally graded piezoelectric energy harvester using thin cylindrical shell, *Int. J. Struct. Stab. Dyn.* **17**(8) (2017) 1–13.
12. L. Librescu, S. Y. Oh and O. Song, Thin-Walled beams made of functionally graded materials and operating in high temperature environment: Vibration and stability, *J. Therm. Stresses* **28**(6) (2005) 649–712.
13. K. Y. Maalawi, Functionally graded bars with enhanced dynamic performance, *J. Mech. Mater. Struct.* **6**(4) (2011) 377–393.
14. E. A. Armanios and A. M. Badir, Free vibration analysis of anisotropic thin-walled closed-section beams, *AIAA J.* **33**(10) (1995) 1905–1910.
15. D. S. Dancila and E. A. Armanios, The influence of coupling on the free vibration of anisotropic thin-walled closed-section beams, *Int. J. Solids Struct.* **35**(23) (1998) 3105–3119.

16. L. Meirovitch, *Principles and Techniques of Vibrations* (Prentice-Hall, Englewood Cliffs, NJ, 1997).
17. I. M. Daniel and O. Ishai, *Engineering Mechanics of Composite Materials*, 2nd edn. (University Press, NewYork, Oxford, 2006).
18. W.-H. Chen and R. F. Gibson, Property distribution determination of non-uniform composite beams from vibration response measurements and Galerkin's method, *J. Appl. Mech.* **65** (1998) 127–133.
19. S.-H. Chi and Y.-L. Chung, Mechanical behavior of functionally graded material plates under transverse load, I: Analysis, *Int. J. Solids Struct.* **43** (2006) 3657–3674.
20. Y. Bedjilili, A. Tounsi, H. M. Berrabah and I. Mechab, Natural frequencies of composite beams with a variable fiber volume fraction including rotary inertia and shear deformation, *Appl. Math. Mech.* **30**(6) (2009) 717–726.
21. L. Librescu and K. Y. Maalawi, Material grading for improved aeroelastic stability of composite wings, *J. Mech. Mater. Struct.* **2**(7) (2007) 1381–1394.
22. K. Shin-Yao, Flutter of rectangular composite plates with variable fiber spacing, *Compos. Struct.* **93** (2011) 2533–2540.
23. K. Y. Maalawi and N. M. El-Chazly, Global optimization of multi-element beam-type structures, in *The Second Int. Conf. Advances in Structural Engineering and Mechanics, ASEM'02* (Busan, South Korea, 21–23 August, 2002).
24. S. Rao, *Engineering Optimization: Theory and Practice*, 4th edn. (John Wiley & Sons, ISBN: 978-0470183526, New York, 2009).
25. P. Venkataraman, *Applied Optimization with MatLab Programming* (John Wiley & Sons, Inc., New York, 2009).
26. J. M. Whitney, Elastic moduli of unidirectional composites with anisotropic filaments, *J. Compos. Mater.* **1** (1967) 188–194.
27. B. Kieback, A. Neubrand and H. Riedal, Processing techniques for functionally graded materials, *Mater. Sci. Eng.* **362** (2003) 81–105.